Published in final edited form as:
J Chem Neuroanat. 2011 October ; 42(2): 102–110. doi:10.1016/j.jchemneu.2011.05.012.

Upregulation of select rab GTPases in cholinergic basal forebrain neurons in mild cognitive impairment and Alzheimer's disease

Stephen D. Ginsberg[1,2,3,*], **Elliott J. Mufson**[5], **Melissa J. Alldred**[1,2], **Scott E. Counts**[5], **Joanne Wuu**[6], **Ralph A. Nixon**[1,2,4], and **Shaoli Che**[1,2]

[1]Center for Dementia Research, Nathan Kline Institute, Orangeburg, NY

[2]Department of Psychiatry, New York University Langone Medical Center, New York, NY

[3]Department of Physiology & Neuroscience, New York University Langone Medical Center, New York, NY

[4]Department of Cell Biology, New York University Langone Medical Center, New York, NY

[5]Department of Neurological Sciences, Rush University Medical Center, Chicago, IL

[6]Department of Neurology, University of Miami Miller School of Medicine, Miami, FL

Abstract

Endocytic system dysfunction is one of the earliest disturbances that occur in Alzheimer's disease (AD), and may underlie the selective vulnerability of cholinergic basal forebrain (CBF) neurons during the progression of dementia. Herein we report that genes regulating early and late endosomes are selectively upregulated within CBF neurons in mild cognitive impairment (MCI) and AD. Specifically, upregulation of *rab4*, *rab5*, *rab7*, and *rab27* was observed in CBF neurons microdissected from postmortem brains of individuals with MCI and AD compared to age-matched control subjects with no cognitive impairment (NCI). Upregulated expression of *rab4*, *rab5*, *rab7*, and *rab27* correlated with antemortem measures of cognitive decline in individuals with MCI and AD. qPCR validated upregulation of these select rab GTPases within microdissected samples of the basal forebrain. Moreover, quantitative immunoblot analysis demonstrated upregulation of rab5 protein expression in the basal forebrain of subjects with MCI and AD. The elevation of *rab4*, *rab5*, and *rab7* expression is consistent with our recent observations in CA1 pyramidal neurons in MCI and AD. These findings provide further support that endosomal pathology accelerates endocytosis and endosome recycling, which may promote aberrant endosomal signaling and neurodegeneration throughout the progression of AD.

Keywords

cognitive decline; endosome; microarray; mild cognitive impairment; rab5; and qPCR

[*]Corresponding Author: Stephen D. Ginsberg, Ph.D., Center for Dementia Research, Nathan Kline Institute, NYU Langone Medical Center, 140 Old Orangeburg Road, Orangeburg, NY 10962, 845-398-2170 (phone), 845-398-5422 (FAX), ginsberg@nki.rfmh.org.

Introduction

Degeneration of cholinergic basal forebrain (CBF) neurons within the nucleus basalis (NB) is a pathological hallmark of Alzheimer's disease (AD) in concert with amyloid deposition, neurofibrillary tangle (NFT) accumulation, and synaptic loss. Notably, CBF neurons are selectively vulnerable to neurodegeneration during the early stages of AD (Cuello *et al.*, 2010; Mufson *et al.*, 2003, 2007a; Whitehouse *et al.*, 1982). Mechanisms underlying the degeneration of the cholinergic neurons within the NB region of the CBF are not well understood. This data is critical for the development of rational therapies for age-related dementing illnesses, including mild cognitive impairment (MCI) and AD.

The endosomal pathway performs a multiplicity of integral functions in neurons including internalizing nutrients and growth factors, recycling receptors, and signaling information to appropriate intracellular pathways (Bishop, 2003; Cataldo *et al.*, 1996; Nixon and Cataldo, 1995). A group of small ras-related GTPase (rab) proteins coordinate trafficking of vesicles from early to late endosomes and other organelles along endosomal-lysosomal pathways (Ng and Tang, 2008; Novick and Brennwald, 1993; Seachrist and Ferguson, 2003; Spang, 2004; Zerial and Stenmark, 1993). Early endosomes receive their contents through endocytosis and target cargoes for vesicular transport via late endosomes to lysosomes, deliver specific cargoes to the Golgi via the retromer, and/or recycle elements to the plasma membrane (Bonanomi *et al.*, 2006; Bronfman *et al.*, 2007). Late endosomes obtain degradative enzymes, including acid hydrolases such as cathepsins, from the trans-Golgi network or by fusion with lysosomal compartments (Bright *et al.*, 2005; Cowles *et al.*, 1997). Endosomes play a crucial role in neuronal development and synaptic transmission (Bronfman *et al.*, 2007; Ibanez, 2007; Salehi *et al.*, 2006; Wang *et al.*, 2007). Moreover, signaling endosomes contain rab GTPases and neurotrophin receptor signaling complexes. For example, the early endosome effector rab5 and late endosome constituent rab7 have been shown in cellular models to regulate nerve growth factor (NGF) signaling (Deinhardt *et al.*, 2006; Liu *et al.*, 2007; Saxena *et al.*, 2005; Valdez *et al.*, 2007). Further, our group has demonstrated that upregulation of rab5 expression downregulates the brain-derived neurotrophic receptor (BDNF) receptor TrkB (Ginsberg *et al.*, 2010a).

Dysfunction of the endosomal system is one of the earliest pathologies observed in the AD brain, as early endosomes in vulnerable forebrain neurons are significantly enlarged compared to control brains (Cataldo *et al.*, 1997, 2001; Nixon *et al.*, 2001). Endosomal alterations precede manifestations of clinical symptoms of AD, intracellular NFT formation, cerebral and vascular amyloid deposition, and are highly selective for AD (Cataldo *et al.*, 2000, 2001; Nixon and Cataldo, 2006; Nixon *et al.*, 2001). In addition, proteins involved in the regulation of endocytosis and early endosomal fusion, including the rab GTPases rab4 and rab5 are increased in expression and altered in location in the AD brain as well as in animal and cellular models of this disease, reflecting an over activation of endocytosis (Grbovic *et al.*, 2003; Mathews *et al.*, 2002; Nixon, 2004). Recently, we observed a selective upregulation of genes regulating early endosomes (*rab4* and *rab5*), late endosomes (*rab7*), and trafficking compartments (*rab24*), among others within CA1 hippocampal pyramidal neurons harvested postmortem from subjects with an antemortem clinical diagnosis of MCI and AD (Ginsberg *et al.*, 2010a). Upregulation of these rab GTPase genes correlate with cognitive decline during AD progression, and hippocampal qPCR and immunoblot analyses confirmed increased levels of these transcripts and their respective encoded proteins, although causality cannot be determined in postmortem human tissues (Ginsberg *et al.*, 2010a, 2010b).

At the molecular and cellular level, endosomal pathway gene dysregulation likely affects survival and maintenance of various forebrain projection systems including the basocortical

cholinergic system, which depend upon retrograde trafficking of members of the NGF family of neurotrophins and their receptors and play a key role in the pathogenic and clinical progression of AD (Bronfman *et al.*, 2007; Mufson *et al.*, 2007a, 2007b). Thus, the regulation of neurotrophin signaling in the forebrain is likely to be dependent upon a multiplicity of factors including specific rab GTPases, among other potential regulators (Ginsberg *et al.*, 2010a). In this regard, single population expression profiling studies from our group demonstrated early down regulation of the NGF, BDNF, and NT3 receptors *TrkA, TrkB, TrkC*, respectively, but not the pan-neurotrophin receptor $p75^{NTR}$ within NB neurons during the progression of AD (Ginsberg *et al.*, 2006b, 2006c) but whether these neurons also display alterations in endosomal-lysosomal gene expression is unknown. Previous studies report an upregulation of select rab GTPases localized to early endosomal, late endosomal, and trafficking compartments within CA1 neurons (Ginsberg *et al.*, 2010a) as well as rab5 and rab7 protein level upregulation in the hippocampus (Ginsberg *et al.*, 2010b), assessment of rab GTPase expression levels within CBF neurons along with coordinated encoded protein expression level assessment is warranted.

As progressive late-onset neurodegenerative disorders such as AD differentially affect neurons throughout the forebrain, assessment of individual populations of vulnerable neurons is highly desirable, as this approach obviates concerns of heterogeneous expression profiles derived from admixed neuronal and non-neuronal cell types (Ginsberg, 2008; Ginsberg *et al.*, 2011; Ginsberg and Mirnics, 2006). Herein, select endosomal markers were assessed within homogeneous populations of NB CBF neurons harvested from subjects who died with a clinical diagnosis of no cognitive impairment (NCI), MCI, or AD using laser capture microdissection (LCM) and custom-designed microarray analysis along with qPCR and immunoblot validation of select genes that were differentially regulated on the microarray platform.

Materials and Methods

Brain tissue

This study was performed under the auspices of Institutional Review Board (IRB) guidelines administrated by the Rush University Medical Center and the Nathan Kline Institute/New York University Langone Medical Center. Clinical and neuropsychological criteria for the Religious Orders Study cohort have been published previously (Bennett *et al.*, 2002; Mufson *et al.*, 2000, 2002). Subjects deemed to be devoid of any comorbid conditions contributing to cognitive impairment were entered into the Religious Orders Study. Antemortem cognitive testing, including the Mini-Mental State Exam (MMSE) and a global cognitive score (GCS) were available within the last year of death. The GCS consists of a battery of 19 neuropsychological tests, providing a composite score for each subject in addition to the individual scores on the respective tests (Arvanitakis *et al.*, 2008; Bennett *et al.*, 2002). A board-certified neurologist designated a clinical diagnosis of NCI {n=11; mean age ± standard deviation (SD) = 81.0 ± 9.6 years}, MCI (n = 10; 81.9 ± 4.3 years), and mild/moderate AD (n = 9; 86.6 ± 4.8 years) for each Religious Orders Study participant (Table I). MCI subjects were defined as individuals with impaired cognitive testing without frank dementia (DeKosky *et al.*, 2002; Mufson *et al.*, 2000), consistent with the clinical classification of MCI adopted by independent research groups (Petersen and Negash, 2008; Reisberg *et al.*, 2008; Winblad *et al.*, 2004).

Tissue blocks containing the substantia innominata which includes the cholinergic neurons of the NB (Mufson *et al.*, 2002, 2003) were obtained at autopsy and immersion-fixed in 4% paraformaldehyde in 0.1 M phosphate buffer, pH 7.2 for 24 hours at 4 °C, paraffin embedded, and sectioned at 6 μm thickness. Adjacent tissue slabs were also snap-frozen in liquid nitrogen for qPCR and immunoblotting studies. A neuropathological diagnosis was

made independent of the clinical diagnosis. Neuropathological designations were based on NIA-Reagan, CERAD, and Braak staging criteria (Braak and Braak, 1991; Hyman and Trojanowski, 1997; Mirra *et al.*, 1991). ApoE genotype and amyloid burden were assessed as described previously (Arvanitakis *et al.*, 2008; Bennett *et al.*, 2004; Braak and Braak, 1991; Counts *et al.*, 2007; Mufson *et al.*, 2000).

Tissue preparation for microarray analysis

Acridine orange histofluorescence (Ginsberg *et al.*, 1997, 1998; Mufson *et al.*, 2002) and bioanalysis (2100, Agilent Biotechnologies, Palo Alto, CA) (Ginsberg *et al.*, 2006a, 2006c; Ginsberg and Mirnics, 2006) were performed on each brain to ensure the presence of high quality RNA. All of the solutions were made with 18.2 mega Ohm RNase-free water (Nanopure Diamond, Barnstead, Dubuque, IA) and RNase-free precautions were used throughout the experimental procedures.

Immunocytochemistry to identify CBF neurons for custom-designed microarray analysis was performed as described previously (Counts *et al.*, 2007, 2008, 2009; Ginsberg *et al.*, 2006a, 2006c). Tissue sections were processed for immunocytochemistry using a monoclonal antibody raised against human $p75^{NTR}$ (Counts *et al.*, 2004; Mufson *et al.*, 1989a, 2002; Schatteman *et al.*, 1988). $p75^{NTR}$ colocalizes with approximately 95% of all CBF neurons within the human NB (Mufson *et al.*, 1989a, 1989b). CBF neurons selected for microaspiration were localized to the anterior subfields of the NB extending from the decussation of the anterior commissure to its emergence at level of the amygdalar complex (Mufson *et al.*, 1989b, 2002). Deparaffinized tissue sections were blocked in a 0.1 M Tris (pH 7.6) solution containing 2% donor horse serum (DHS; Sigma, St. Louis, MO) and 0.01% Triton X-100 for 1 hour and then incubated with the primary antibody (Neomarkers, Fremont, CA; 1:20,000 dilution) in a 0.1 M Tris/2% DHS solution overnight at 4 °C in a humidified chamber. Sections were processed with the ABC kit (Vector Labs, Burlingame, CA) and developed with 0.05% diaminobenzidine (Sigma), 0.03% hydrogen peroxide, and 0.01 M imidazole in Tris buffer for 10 minutes (Counts *et al.*, 2009; Ginsberg *et al.*, 2006a, 2006c, 2010a). Tissue sections were not coverslipped or counterstained and maintained in RNase-free 0.1 M Tris for LCM.

LCM and Terminal Continuation (TC) RNA amplification

LCM and TC RNA amplification procedures have been described in detail (Alldred *et al.*, 2008, 2009; Che and Ginsberg, 2004; Ginsberg, 2005, 2008; Ginsberg *et al.*, 2010a). CBF neurons from the NB were microaspirated via LCM (Arcturus PixCell IIe, Applied Biosystems, Foster City, CA) as described previously (Counts *et al.*, 2008, 2009; Ginsberg *et al.*, 2006b, 2010a). Approximately 25 cells were captured per reaction for population cell analysis. A total of 3-8 reactions (containing 50 LCM-captured CBF neurons each) were performed per human brain. Linearity and reproducibility of the TC RNA amplification procedure has been published previously, including the use of CBF neurons as input sources of RNA (Alldred *et al.*, 2008, 2009; Che and Ginsberg, 2004; Ginsberg, 2008). The TC RNA amplification protocol is available at http://cdr.rfmh.org/pages/ginsberglabpage.html. LCM-captured CBF neurons were homogenized in 500 μl of Trizol reagent (Invitrogen), chloroform extracted, and isopropanol precipitated (Alldred *et al.*, 2009). RNAs were reverse transcribed in a solution containing a poly d(T) primer (100 ng/μl) and TC primer (100 ng/μl) in 1X first strand buffer (Invitrogen), 2 μg of linear acrylamide (Applied Biosystems), 10 mM dNTPs, 100 μM dithiothreitol (DTT), 20 U of SuperRNase Inhibitor (Applied Biosystems) and 200 U of reverse transcriptase (Superscript III, Invitrogen). Single stranded cDNAs were digested and then placed in a thermal cycler in a solution consisting of 10 mM Tris (pH 8.3), 50 mM KCl, 1.5 mM $MgCl_2$, and 10 U RNase H (Invitrogen) in a final volume of 100 μl. The thermal cycler program was set as follows: RNase H digestion

at 37 °C, 30 minutes; denaturation at 95 °C, 3 minutes; and primer re-annealing at 60 °C, 5 minutes. Samples were purified by column filtration (Montage, Millipore, Billerica, MA). Hybridization probes were synthesized by *in vitro* transcription using ^{33}P incorporation in 40 mM Tris (pH 7.5), 6 mM $MgCl_2$, 10 mM NaCl, 2 mM spermidine, 10 mM DTT, 2.5 mM ATP, GTP and CTP, 100 μM of cold UTP, 20 U of RNase inhibitor, 2 KU of T7 RNA polymerase (Epicentre, Madison, WI), and 120 μCi of ^{33}P-UTP (Perkin-Elmer, Boston, MA) (Alldred *et al.*, 2009; Ginsberg, 2008). The reaction was performed at 37 °C for 4 hours. Radiolabeled TC RNA probes were hybridized to custom-designed cDNA arrays without further purification.

Custom-designed array platforms and hybridization

Array platforms consisted of 1 μg of linearized cDNA purified from plasmid preparations adhered to high-density nitrocellulose (Hybond XL, GE Healthcare, Piscataway, NJ). Each cDNA and/or expressed sequence-tagged cDNA (EST) was verified by restriction digestion and sequence analysis. Human and select mouse clones were employed on the custom-designed array. Notably, all of the rab GTPases and related endosomal-lysosomal-autophagic genes were derived from human sequences. Approximately 576 cDNAs/ESTs were utilized on the current array platform. The majority of genes are represented by one transcript on the array platform.

Arrays were prehybridized (2 hours) and hybridized (12 hours) in a solution consisting of 6X saline–sodium phosphate–ethylenediaminetetraacetic acid (SSPE), 5X Denhardt's solution, 50% formamide, 0.1% sodium dodecyl sulfate (SDS), and denatured salmon sperm DNA (200 μg/ml) at 42 °C in a rotisserie oven (Ginsberg, 2005, 2008). Following hybridization, arrays were washed sequentially in 2X SSC/0.1% SDS, 1X SSC/0.1% SDS and 0.5X SSC/0.1% SDS for 15 min each at 37 °C and placed in a phosphor screen for 24 hours. Arrays were developed on a phosphor imager (GE Healthcare). All array images were adjusted to the same brightness and contrast levels for data acquisition and analysis.

Statistical analysis for the microarray study

Procedures for custom-designed microarray analysis have been described in detail (Alldred *et al.*, 2008, 2009; Ginsberg, 2008; Ginsberg *et al.*, 2006b, 2006c, 2010a; Ginsberg and Mirnics, 2006). Briefly, expression of TC amplified RNA bound to each linearized cDNA minus background was expressed as a ratio of the total hybridization signal intensity of the array. This global normalization approach does not allow the absolute quantitation of mRNA levels. However, an expression profile of relative changes in mRNA levels was generated (Eberwine *et al.*, 2001; Ginsberg, 2005, 2008). Clinical and demographic characteristics were compared among clinical diagnostic groups by one-way analysis of variance (ANOVA) or Fisher's exact test and neuropathologic classifications were compared by Kruskal-Wallis test. Bonferroni correction was employed for multiple comparisons. Associations between gene expression levels and case characteristics including diagnostic groups, demographic, clinical, and neuropathological variables was evaluated via mixed models repeated measures analyses with random intercept, fixed effect covariate, equal variance assumption, Kenward-Roger denominator degrees of freedom, and unstructured covariance structure (SAS Institute Inc, 2009). In cases where at least one variance component was estimated to be zero, analyses were performed with the term for random intercept removed from the model. For graphical presentations, the mean expression level of each case was plotted. The level of statistical significance was set at 0.01 (two-sided) to account for the large number of analyses performed.

qPCR

qPCR was performed on frozen micropunches of the basal forebrain containing the NB from NCI (n= 11), MCI (n= 8), and mild/moderate and severe AD (n= 8) Religious Orders Study cases. Five of these cases were also included in the microarray experiment. See Supplemental Table I for demographic information and neuropathological assessment of the cases used for qPCR. Taqman (Applied Biosystems) qPCR primers were employed for the following genes: *rab4* (Hs01106488_m1), *rab5* (Hs00991293_g1), *rab7* (Hs01115139_m1), *rab24* (Hs01585713_g1), *rab27* (Hs00608302_m1), and the housekeeping gene *Gapdh* (Hs02758991_g1). Assays were performed on a real-time PCR cycler (7900HT, Applied Biosystems) in 96-well optical plates with caps (Alldred *et al.*, 2008, 2009; Devi *et al.*, 2010; Kaur *et al.*, 2010). The ddCT method was employed to determine relative gene level differences with *Gapdh* qPCR products used as a control (ABI, 2004; Alldred *et al.*, 2009; Devi *et al.*, 2010; Kaur *et al.*, 2010). qPCR assessments were run in triplicate for each case. Variance component analyses demonstrated that the within-case variability was sufficiently small. Therefore, the triplicate average was computed for each case and used in subsequent analyses. Alterations in PCR product synthesis were compared across diagnostic groups by Kruskal-Wallis test, with Bonferroni correction for post-hoc comparisons. Associations between qPCR expression levels and cognitive measures or neuropathological criteria were assessed by Spearman rank correlation or Wilcoxon rank-sum test. The level of statistical significance was set at 0.05 (two-sided).

Immunoblot analysis

Frozen basal forebrain samples microdissected from NCI (n= 18), MCI (n= 10), and mild/moderate and severe AD (n= 19) brains were obtained from four brain banks (see Supplemental Table II for case demographics and neuropathological characterization). The 5 Religious Orders Study cases with tissue available for both the microarray and qPCR experiments were also included in the immunoblot analysis. Samples were homogenized in a 20 mM Tris-HCl (pH 7.4) buffer containing 10% (w/v) sucrose, 1 mM ethylenediaminetetraacetic acid (EDTA), 5 mM ethylene glycol-bis (ß-aminoethylether)-N, N, N’, N’-tetra-acetic acid (EGTA), 2 mg/ml of the following: (aprotinin, leupeptin, and chymostatin), 1 mg/ml of the following: {pepstatin A, antipain, benzamidine, and phenylmethylsulfonyl fluoride (PMSF)}, 100 μg/ml of the following: {soybean trypsin inhibitor, Na-p-tosyl-L-lysine chloromethyl ketone (TLCK), and N-tosyl-L-phenylalanine chloromethyl ketone (TPCK)}, 1 mM of the following: (sodium fluoride and sodium orthovanadate) and centrifuged as described previously (Counts *et al.*, 2004; Ginsberg *et al.*, 2010a, 2010b). All protease inhibitors were purchased from Sigma (St. Louis, MO). Homogenates (10 μg) were subjected to sodium dodecyl sulfate-polyacrylamide gel electrophoresis (SDS-PAGE; 4-15% gradient acrylamide gels; Bio-Rad, Hercules, CA), and transferred to nitrocellulose by electroblotting (Mini Transblot, Bio-Rad). Nitrocellulose membranes were placed in blocking buffer (LiCor, Lincoln, NE) for 1 hour at 4 °C prior to being incubated with antibodies directed against rab5 (rab5A; rabbit polyclonal sc-309; Santa Cruz Biotechnology, Santa Cruz, CA; 1:1,000 dilution), rab7 (rabbit polyclonal sc-10767; Santa Cruz Biotechnology 1:1,000 dilution), or ß-tubulin (TUBB; monoclonal antibody; Sigma, 1:1,000 dilution) in blocking buffer overnight at 4 °C. Membranes were developed using affinity–purified secondary antibodies conjugated to IRDye 800 (Rockland, Gilbertsville, PA), visualized using an infrared detection system (Odyssey, LiCor), and immunoblots quantified by densitometric software supplied by the manufacturer. rab5-immunoreactive and rab7-immunoreactive bands were normalized to TUBB immunoreactivity. Differences in immunoreactive band intensity were compared across diagnostic groups by Kruskal-Wallis test, with Bonferroni correction for post-hoc comparisons. Associations between protein levels and clinical, demographic, and

neuropathological variables were assessed by Spearman rank correlation or Wilcoxon rank-sum test. The level of statistical significance was set at 0.05 (two-sided).

Results

Clinical and neuropathological characteristics

In all three experiments (microarray, qPCR, and immunoblot analysis), age, gender, educational level, and postmortem interval (PMI) were comparable across the three clinical diagnostic groups (Table I and Supplemental Tables I and II). Distribution of Braak scores was significantly different across clinical conditions, with NCI having lower Braak scores than AD and the Braak scores of MCI between those of NCI and AD (Table I and Supplemental Tables I and II). NIA-Reagan diagnosis and CERAD diagnosis, which were available for the microarray and qPCR cases, differentiated NCI from AD (see Table I and Supplemental Table I).

Microarray analysis of select rab GTPases in CBF neurons

Datasets were generated by expression profiling 174 NB LCM population cell captures (with a median of 5 and a range of 3-11 cells per case) via custom-designed microarray analysis. Results identified differential regulation of several rab GTPases, including significant up regulation of early endosome effectors *rab4* ($p < 0.0008$; AD>NCI & MCI) and *rab5* ($p < 0.0001$; AD & MCI>NCI), late endosome constituent *rab7* ($p < 0.0002$; AD & MCI>NCI), and the exocytic secretion pathway molecule *rab27* ($p < 0.002$; AD>NCI) (Fig. 1 and Table II). Alterations in *rab5* and *rab7* expression were considered early changes, as upregulation was observed in MCI and AD, *rab27* upregulation in MCI was considered intermediate between NCI and AD, whereas upregulation of *rab4* appeared as a later alteration, since significant changes were found in AD, but not MCI, consisent with our previous observations in CA1 pyramidal neurons (Ginsberg *et al.*, 2010a). Despite the suggestion of a trend (e.g., for downregulation of the synaptic-related marker *rab3*), no statistically significant differential regulation was observed for *rab1, rab2, rab3, rab6, rab10*, or *rab24* (Table II). Moreover, expression profiling of select rab GTPases in postmortem NB neurons correlated with antemortem cognitive measures. Strong negative associations were found between GCS performance and *rab4* ($p < 0.02$), *rab5* ($p < 0.004$), *rab7* ($p < 0.006$), and *rab27* ($p < 0.004$) NB neuron expression levels (Fig. 2). Similar associations were also observed between MMSE and these CBF neuron expression levels (data not shown). Higher Braak scores were associated with upregulation of *rab5* ($p < 0.01$), *rab7* ($p < 0.008$), and *rab27* ($p < 0.04$) in CBF neurons.

qPCR validation of microarray data

Select rab GTPase gene expression levels were evaluated via qPCR using micropunches of frozen basal forebrain obtained from NCI, MCI, and AD cases. qPCR analysis independently validated the microarray findings, including upregulation of *rab4, rab5, rab7*, and *rab27* and no changes in *rab24* expression (Table III). Similar to the microarray observations, correlation of basal forebrain qPCR product levels with antemortem cognitive measures and neuropathological criteria indicated significant negative association between GCS performance with *rab4* ($p < 0.0006$), *rab5* ($p < 0.0001$), *rab7* ($p < 0.0001$), and *rab27* ($p < 0.04$) basal forebrain expression levels. Similar correlations were observed between MMSE scores and *rab4, rab5, rab7*, and *rab27* expression levels. Basal forebrain rab GTPase upregulation also correlated with Braak scores, NIA-Reagan diagnosis, and CERAD diagnosis for *rab4* (Braak, $p < 0.02$; NIA-Reagan, $p < 0.005$; CERAD, $p < 0.03$), *rab5* (Braak, $p < 0.0005$; NIA-Reagan, $p < 0.002$; CERAD, $p < 0.01$), *rab7* (Braak, $p < 0.002$; NIA-Reagan, $p < 0.0004$; CERAD, $p < 0.03$), and *rab27* (Braak, $p < 0.002$; NIA-Reagan, $p < 0.002$; CERAD, $p < 0.02$).

Immunoblot assessment of rab5 and rab7 in the basal forebrain

Immunoblot analysis using basal forebrain homogenates identified an ~27 kDa band with the rab5 antibody and an ~25 kDa band with the rab7 antibody. Quantitative analysis demonstrated a significant upregulation of rab5 ($p < 0.02$; AD & MCI>NCI) indicative of an early alteration, whereas comparison of rab7 expression among clinical diagnostic groups did not reach statistical significance (Table IV). Upregulation of basal forebrain rab5 expression also correlated with Braak staging ($p < 0.002$).

Discussion

An overall goal of our expression profiling studies is to identify mechanisms that underlie selective vulnerability of specific neurons and fucntional circuits during the progression of AD. In the present study we applied this approach at the level of homogeneous neuronal populations to evaluate vulnerable cholinergic neurons within the NB subfield of the CBF. Simultaneous quantitative assessment of multiple rab GTPase mRNAs by LCM, TC RNA amplification, and custom-designed microarray analysis combined with qPCR and immunoblot validation strategies provides a paradigm whereby CBF neurons can be differentiated from adjacent neuronal and non-neuronal populations (Che and Ginsberg, 2004; Ginsberg, 2008; Ginsberg *et al.*, 2006c; Mufson *et al.*, 2008). Importantly, the experimental design enables postmortem quantitative analyses of vulnerable CBF neurons in subjects at different stages of clinical impairment and facilitates comparisons with antemortem cognitive measures from the same subjects (Counts *et al.*, 2007; Galvin and Ginsberg, 2005; Ginsberg *et al.*, 2006c, 2010a). Results indicate endosomal dysfunction occurs within the cholinergic neurons of the NB during prodromal AD. Expression profiling revealed significant upregulation of early endosome effector genes including *rab4* and *rab5*, the late endosome gene *rab7*, and exocytic pathway gene *rab27* as AD progresses. Importantly, upregulation of these select rab GTPases correlated with cognitive decline and neuropathological criteria for AD. These findings are similar to those found within CA1 pyramidal neurons,where an upregulation of *rab4*, *rab5*, and *rab7* were observed (Ginsberg *et al.*, 2010a), consistent with the present report. Interestingly, the trafficking marker *rab24* was upregulated in CA1 pyramidal neurons, whereas *rab27* was not differentially regulated (Ginsberg *et al.*, 2010a), which may reflect the intrinsic properties of these two different cell types.

The present results are consistent with a growing body of literature in human postmortem material and in animal and cellular models of AD and Down's syndrome (DS) that indicate over activation of the endosomal pathway occurs early in the progression of the disease process. Current findings confirm and extend previous morphological, molecular, and cellular datasets demonstrating enlarged endosomes and upregulation of select rab GTPases in AD (Cataldo *et al.*, 1996, 2000, 2008; Ginsberg *et al.*, 2010a; Grbovic *et al.*, 2003; Nixon and Cataldo, 2006). Specifically, overexpression of rab5 causes enlarged endosomes, one of the earliest pathological alterations observed in AD, and rab5 upregulation is found in vulnerable hippocampal and basal forebrain regions, but not in the relatively spared striatum and cerebellum in MCI and AD (Cataldo *et al.*, 2000, 2001, 2008; Ginsberg *et al.*, 2010b). The present novel finding of *rab27* upregulation is consistent with exosome secretion abnormalities in AD (Ghidoni *et al.*, 2009; Gomi *et al.*, 2007; Ostrowski *et al.*, 2010), and may point to a link in defective TrkB trafficking through interactions with rab27 on signaling endosomes (Arimura *et al.*, 2009).

Without proper expression and maintenance of neurotrophin receptors, principally TrkA and the pan-neurotrophin receptor $p75^{NTR}$ within CBF neurons, cholinotrophic forebrain circuits critically important for mnemonic and executive function are at risk for neurodegeneration (Boissiere *et al.*, 1997; Chu *et al.*, 2001; Ginsberg *et al.*, 2006c; Mufson *et al.*, 2007b, 2008).

The regulation of neurotrophin signaling in the forebrain is likely to be dependent upon a multiplicity of factors including specific rab GTPases. Indeed, our previous single cell research has demonstrated early down regulation of *TrkA*, *TrkB*, *TrkC*, but not $p75^{NTR}$ within CBF neurons of the NB during the progression of AD (Ginsberg *et al.*, 2006b, 2006c). We cannot exclude the possibility that other factors, such as gender, immunological responses, epigenetic alterations, and environmental exposures (Chouliaras *et al.*, 2010; Coppede and Migliore, 2010; Counts *et al.*, 2011; Licastro and Chiappelli, 2003), as well as additional classes of transcripts and their encoded proteins are involved in neurodegenerative programs within vulnerable populations, such as CBF neurons, within MCI and AD brains including glutamate receptor subunits, synaptic-related markers, energy and metabolism related markers, and apoptotic signaling genes, among others (Blalock *et al.*, 2004; Colangelo *et al.*, 2002; Liang *et al.*, 2007, 2008). Notwithstanding these caveats, interrelationships between retrograde endosomal trafficking of neurotrophin/neurotrophin receptor complexes are well documented, particularly within the basal forebrain cholinergic neuronal system with NGF and BDNF binding to, and trafficking with TrkA, TrkB, and $p75^{NTR}$ (Arimura *et al.*, 2009; Bronfman *et al.*, 2007; Howe and Mobley, 2004; Valdez *et al.*, 2007). Interestingly, *in vitro* studies indicate that rab5 overexpression downregulates TrkB (Ginsberg *et al.*, 2010a). This observation together with our findings of rab5 gene and protein upregulation in both CA1 pyramidal and CBF neurons suggest a mechanistic interaction associated with neuronal vulnerability. The endosomal system is also perturbed in relevant animal models, including the Ts65Dn mouse model of DS and AD, with amyloid-beta precursor protein (APP) being required for the manifestation of the early endosome enlargement phenotype (Cataldo *et al.*, 2003; Salehi *et al.*, 2006). These finding suggest an interaction between *App* gene dosage, APP processing, and APP metabolites of this regulatory circuit with the endosomal system. rab GTPase-mediated regulation of endocytosis is critical for synaptic plasticity associated with learning and memory (Ng and Tang, 2008; Nixon, 2004), as well as with cellular degradative pathways shown to be dysfunctional in the AD brain (Nixon *et al.*, 2000, 2008). Importantly, rab5, rab7, and rab27 regulate endocytic sorting within axonal retrograde transport pathways (Arimura *et al.*, 2009; Deinhardt *et al.*, 2006).

The present expression profiling results within homogeneous populations of NB CBF neurons indicate the importance of evaluating rab GTPases and other endosomal-lysosomal-autophagic markers within vulnerable cell types in MCI and AD. Within the context of our ongoing profiling studies of NB CBF neurons across different stages of cognitive impairment (NCI, MCI, and AD), upregulation of select rab GTPases is found along with dysregulation of several other relevant markers, including upregulation of α7 nicotinic acetylcholine receptor (CHRNA7) and matrix metalloproteinase 9 (MMP-9) expression (Bruno *et al.*, 2009; Counts *et al.*, 2007), an increase in the ratio of proNGF to the mature NGF peptide (Mufson *et al.*, 2007b; Peng *et al.*, 2004), and galanin fiber hyperinnervation in CBF neurons (Counts *et al.*, 2006, 2008, 2009) (Fig. 3). By contrast, downregulation of TrkA, TrkB, TrkC, and BDNF (both proBDNF and the mature peptide) is also observed within NB CBF neurons (Ginsberg *et al.*, 2006b, 2006c; Peng *et al.*, 2005), along with a shift in the 3-repeat tau/4-repeat tau ratio (Ginsberg *et al.*, 2006a), providing a dynamic regulation of genes and encoded proteins that may be a fingerprint of selective vulnerability (Fig. 3). Also, several genes and encoded proteins that are relevant to the cholinergic phenotype of CBF neurons do not appear to be altered in AD (with the possible exception of end-stage disease), including $p75^{NTR}$, sortilin, and choline acetyltransferase (ChAT) (Ginsberg *et al.*, 2006b, 2006c; Mufson *et al.*, 2002, 2010), although potential gender differences within $p75^{NTR}$ expression are now being recognized (Counts *et al.*, 2011). We conclude that over activation of select early and late endocytic as well as exocytic rab GTPases contribute to CBF neurodegeneration, in part, by impairing neurotrophin receptor

signaling and that these genes are early molecular markers for the development of MCI and AD.

Supplementary Material

Refer to Web version on PubMed Central for supplementary material.

Acknowledgments

Support for this project comes from NIH grants AG17617, AG14449, and AG09466, and the Alzheimer's Association. We thank Irina Elarova, Shaona Fang, Arthur Saltzman for expert technical assistance and those members of the Rush Alzheimer's Disease Center and those who participate in the Religious Orders Study. A list of contributing groups can be found at the website: http://www.rush.edu/rumc/page-R12394.html.

References

ABI. Guide to Performing Relative Quantitation of Gene Expression Using Real-Time Quantitative PCR. Applied Biosystems Product Guide. 2004:1–60.

Alldred MJ, Che S, Ginsberg SD. Terminal continuation (TC) RNA amplification enables expression profiling using minute RNA input obtained from mouse brain. Int J Mol Sci. 2008; 9:2091–2104. [PubMed: 19165351]

Alldred MJ, Che S, Ginsberg SD. Terminal continuation (TC) RNA amplification without second strand synthesis. J Neurosci Methods. 2009; 177:381–385. [PubMed: 19026688]

Arimura N, Kimura T, Nakamuta S, Taya S, Funahashi Y, Hattori A, Shimada A, Menager C, Kawabata S, Fujii K, Iwamatsu A, Segal RA, Fukuda M, Kaibuchi K. Anterograde transport of TrkB in axons is mediated by direct interaction with Slp1 and Rab27. Dev Cell. 2009; 16:675–686. [PubMed: 19460344]

Arvanitakis Z, Grodstein F, Bienias JL, Schneider JA, Wilson RS, Kelly JF, Evans DA, Bennett DA. Relation of NSAIDs to incident AD, change in cognitive function, and AD pathology. Neurology. 2008; 70:2219–2225. [PubMed: 18519870]

Bennett DA, Schneider JA, Wilson RS, Bienias JL, Arnold SE. Neurofibrillary tangles mediate the association of amyloid load with clinical Alzheimer disease and level of cognitive function. Arch Neurol. 2004; 61:378–384. [PubMed: 15023815]

Bennett DA, Wilson RS, Schneider JA, Evans DA, Beckett LA, Aggarwal NT, Barnes LL, Fox JH, Bach J. Natural history of mild cognitive impairment in older persons. Neurology. 2002; 59:198–205. [PubMed: 12136057]

Bishop NE. Dynamics of endosomal sorting. Int Rev Cytol. 2003; 232:1–57. [PubMed: 14711115]

Blalock EM, Geddes JW, Chen KC, Porter NM, Markesbery WR, Landfield PW. Incipient Alzheimer's disease: microarray correlation analyses reveal major transcriptional and tumor suppressor responses. Proc Natl Acad Sci U S A. 2004; 101:2173–2178. [PubMed: 14769913]

Boissiere F, Faucheux B, Ruberg M, Agid Y, Hirsch EC. Decreased TrkA gene expression in cholinergic neurons of the striatum and basal forebrain of patients with Alzheimer's disease. Exp Neurol. 1997; 145:245–252. [PubMed: 9184126]

Bonanomi D, Benfenati F, Valtorta F. Protein sorting in the synaptic vesicle life cycle. Prog Neurobiol. 2006; 80:177–217. [PubMed: 17074429]

Braak H, Braak E. Neuropathological stageing of Alzheimer-related changes. Acta Neuropathol. 1991; 82:239–259. [PubMed: 1759558]

Bright NA, Gratian MJ, Luzio JP. Endocytic delivery to lysosomes mediated by concurrent fusion and kissing events in living cells. Curr Biol. 2005; 15:360–365. [PubMed: 15723798]

Bronfman FC, Escudero CA, Weis J, Kruttgen A. Endosomal transport of neurotrophins: roles in signaling and neurodegenerative diseases. Dev Neurobiol. 2007; 67:1183–1203. [PubMed: 17514710]

Bruno MA, Mufson EJ, Wuu J, Cuello AC. Increased matrix metalloproteinase 9 activity in mild cognitive impairment. J Neuropathol Exp Neurol. 2009; 68:1309–1318. [PubMed: 19915485]

Cataldo A, Rebeck GW, Ghetri B, Hulette C, Lippa C, Van Broeckhoven C, van Duijn C, Cras P, Bogdanovic N, Bird T, Peterhoff C, Nixon R. Endocytic disturbances distinguish among subtypes of Alzheimer's disease and related disorders. Ann Neurol. 2001; 50:661–665. [PubMed: 11706973]

Cataldo AM, Barnett JL, Picroni C, Nixon RA. Increased neuronal endocytosis and protease delivery to early endosomes in sporadic Alzheimer's disease: neuropathologic evidence for a mechanism of increased ß-amyloidogenesis. J. Neurosci. 1997; 17:6142–6151. [PubMed: 9236226]

Cataldo AM, Hamilton DJ, Barnett JL, Paskevich PA, Nixon RA. Properties of the endosomal-lysosomal system in the human central nervous system: disturbances mark most neurons in populations at risk to degenerate in Alzheimer's disease. J. Neurosci. 1996; 16:186–199. [PubMed: 8613784]

Cataldo AM, Mathews PM, Boiteau AB, Hassinger LC, Peterhoff CM, Jiang Y, Mullaney K, Neve RL, Gruenberg J, Nixon RA. Down syndrome fibroblast model of Alzheimer-related endosome pathology: accelerated endocytosis promotes late endocytic defects. Am J Pathol. 2008; 173:370–384. [PubMed: 18535180]

Cataldo AM, Petanceska S, Peterhoff CM, Terio NB, Epstein CJ, Villar A, Carlson EJ, Staufenbiel M, Nixon RA. App gene dosage modulates endosomal abnormalities of Alzheimer's disease in a segmental trisomy 16 mouse model of Down syndrome. J Neurosci. 2003; 23:6788–6792. [PubMed: 12890772]

Cataldo AM, Peterhoff CM, Troncoso JC, Gomez-Isla T, Hyman BT, Nixon RA. Endocytic pathway abnormalities precede amyloid beta deposition in sporadic Alzheimer's disease and Down syndrome: differential effects of APOE genotype and presenilin mutations. Am J Pathol. 2000; 157:277–286. [PubMed: 10880397]

Che S, Ginsberg SD. Amplification of transcripts using terminal continuation. Lab Invest. 2004; 84:131–137. [PubMed: 14647400]

Chouliaras L, Rutten BP, Kenis G, Peerbooms O, Visser PJ, Verhey F, van Os J, Steinbusch HW, van den Hove DL. Epigenetic regulation in the pathophysiology of Alzheimer's disease. Prog Neurobiol. 2010; 90:498–510. [PubMed: 20097254]

Chu Y, Cochran EJ, Bennett DA, Mufson EJ, Kordower JH. Down-regulation of trkA mRNA within nucleus basalis neurons in individuals with mild cognitive impairment and Alzheimer's disease. J Comp Neurol. 2001; 437:296–307. [PubMed: 11494257]

Colangelo V, Schurr J, Ball MJ, Pelaez RP, Bazan NG, Lukiw WJ. Gene expression profiling of 12633 genes in Alzheimer hippocampal CA1: transcription and neurotrophic factor down-regulation and up-regulation of apoptotic and pro-inflammatory signaling. J Neurosci Res. 2002; 70:462–473. [PubMed: 12391607]

Coppede F, Migliore L. Evidence linking genetics, environment, and epigenetics to impaired DNA repair in Alzheimer's disease. J Alzheimers Dis. 2010; 20:953–966. [PubMed: 20182042]

Counts SE, Che S, Ginsberg SD, Mufson EJ. Gender differences in neurotrophin and glutamate receptor expression in cholinergic nucleus basalis neurons during the progression of Alzheimer's disease. J Chem Neuroanat. 2011 in press.

Counts SE, Chen EY, Che S, Ikonomovic MD, Wuu J, Ginsberg SD, Dekosky ST, Mufson EJ. Galanin fiber hypertrophy within the cholinergic nucleus basalis during the progression of Alzheimer's disease. Dement Geriatr Cogn Disord. 2006; 21:205–214. [PubMed: 16410678]

Counts SE, He B, Che S, Ginsberg SD, Mufson EJ. Galanin hyperinnervation upregulates choline acetyltransferase expression in cholinergic basal forebrain neurons in Alzheimer's disease. Neurodegener Dis. 2008; 5:228–331. [PubMed: 18322398]

Counts SE, He B, Che S, Ginsberg SD, Mufson EJ. Galanin fiber hyperinnervation preserves neuroprotective gene expression in cholinergic basal forebrain neurons in Alzheimer's disease. J Alzheimers Dis. 2009; 18:885–896. [PubMed: 19749437]

Counts SE, He B, Che S, Ikonomovic MD, Dekosky ST, Ginsberg SD, Mufson EJ. {alpha}7 Nicotinic receptor up-regulation in cholinergic basal forebrain neurons in Alzheimer disease. Arch Neurol. 2007; 64:1771–1776. [PubMed: 18071042]

Counts SE, Nadeem M, Wuu J, Ginsberg SD, Saragovi HU, Mufson EJ. Reduction of cortical TrkA but not p75(NTR) protein in early-stage Alzheimer's disease. Ann Neurol. 2004; 56:520–531. [PubMed: 15455399]

Cowles CR, Odorizzi G, Payne GS, Emr SD. The AP-3 adaptor complex is essential for cargo-selective transport to the yeast vacuole. Cell. 1997; 91:109–118. [PubMed: 9335339]

Cuello AC, Bruno MA, Allard S, Leon W, Iulita MF. Cholinergic involvement in Alzheimer's disease. A link with NGF maturation and degradation. J Mol Neurosci. 2010; 40:230–235. [PubMed: 19680822]

Deinhardt K, Salinas S, Verastegui C, Watson R, Worth D, Hanrahan S, Bucci C, Schiavo G. Rab5 and rab7 control endocytic sorting along the axonal retrograde transport pathway. Neuron. 2006; 52:293–305. [PubMed: 17046692]

DeKosky ST, Ikonomovic MD, Styren SD, Beckett L, Wisniewski S, Bennett DA, Cochran EJ, Kordower JH, Mufson EJ. Upregulation of choline acetyltransferase activity in hippocampus and frontal cortex of elderly subjects with mild cognitive impairment. Ann Neurol. 2002; 51:145–155. [PubMed: 11835370]

Devi L, Alldred MJ, Ginsberg SD, Ohno M. Sex- and brain region-specific acceleration of beta-amyloidogenesis following behavioral stress in a mouse model of Alzheimer's disease. Mol Brain. 2010; 3:34. [PubMed: 21059265]

Eberwine J, Kacharmina JE, Andrews C, Miyashiro K, McIntosh T, Becker K, Barrett T, Hinkle D, Dent G, Marciano P. mRNA expression analysis of tissue sections and single cells. J Neurosci. 2001; 21:8310–8314. [PubMed: 11606616]

Galvin JE, Ginsberg SD. Expression profiling in the aging brain: A perspective. Ageing Res Rev. 2005; 4:529–547. [PubMed: 16249125]

Ghidoni R, Paterlini A, Albertini V, Glionna M, Monti E, Schiaffonati L, Benussi L, Levy E, Binetti G. Cystatin C is released in association with exosomes: A new tool of neuronal communication which is unbalanced in Alzheimer's disease. Neurobiol Aging. 2009 in press.

Ginsberg SD. RNA amplification strategies for small sample populations. Methods. 2005; 37:229–237. [PubMed: 16308152]

Ginsberg SD. Transcriptional profiling of small samples in the central nervous system. Methods Mol Biol. 2008; 439:147–158. [PubMed: 18370101]

Ginsberg SD, Alldred MJ, Che S. Gene expression levels assessed by CA1 pyramidal neuron and regional hippocampal dissections in Alzheimer's disease. Submitted for publication. 2011

Ginsberg SD, Alldred MJ, Counts SE, Cataldo AM, Neve RL, Jiang Y, Wuu J, Chao MV, Mufson EJ, Nixon RA, Che S. Microarray analysis of hippocampal CA1 neurons implicates early endosomal dysfunction during Alzheimer's disease progression. Biol Psychiatry. 2010a; 68:885–893. [PubMed: 20655510]

Ginsberg SD, Che S, Counts SE, Mufson EJ. Shift in the ratio of three-repeat tau and four-repeat tau mRNAs in individual cholinergic basal forebrain neurons in mild cognitive impairment and Alzheimer's disease. J Neurochem. 2006a; 96:1401–1408. [PubMed: 16478530]

Ginsberg SD, Che S, Counts SE, Mufson EJ. Single cell gene expression profiling in Alzheimer's disease. NeuroRx. 2006b; 3:302–318. [PubMed: 16815214]

Ginsberg SD, Che S, Wuu J, Counts SE, Mufson EJ. Down regulation of trk but not p75NTR gene expression in single cholinergic basal forebrain neurons mark the progression of Alzheimer's disease. J Neurochem. 2006c; 97:475–487. [PubMed: 16539663]

Ginsberg SD, Crino PB, Lee VM, Eberwine JH, Trojanowski JQ. Sequestration of RNA in Alzheimer's disease neurofibrillary tangles and senile plaques. Ann Neurol. 1997; 41:200–209. [PubMed: 9029069]

Ginsberg SD, Galvin JE, Chiu TS, Lee VM, Masliah E, Trojanowski JQ. RNA sequestration to pathological lesions of neurodegenerative diseases. Acta Neuropathol. 1998; 96:487–494. [PubMed: 9829812]

Ginsberg SD, Mirnics K. Functional genomic methodologies. Prog Brain Res. 2006; 158:15–40. [PubMed: 17027690]

Ginsberg SD, Mufson EJ, Counts SE, Wuu J, Alldred MJ, Nixon RA, Che S. Regional selectivity of rab5 and rab7 protein upregulation in mild cognitive impairment and Alzheimer's disease. J Alzheimers Dis. 2010b; 22:631–639. [PubMed: 20847427]

Gomi H, Mori K, Itohara S, Izumi T. Rab27b is expressed in a wide range of exocytic cells and involved in the delivery of secretory granules near the plasma membrane. Mol Biol Cell. 2007; 18:4377–4386. [PubMed: 17761531]

Grbovic OM, Mathews PM, Jiang Y, Schmidt SD, Dinakar R, Summers-Terio NB, Ceresa BP, Nixon RA, Cataldo AM. Rab5-stimulated up-regulation of the endocytic pathway increases intracellular beta-cleaved amyloid precursor protein carboxyl-terminal fragment levels and Abeta production. J Biol Chem. 2003; 278:31261–31268. [PubMed: 12761223]

Howe CL, Mobley WC. Signaling endosome hypothesis: A cellular mechanism for long distance communication. J Neurobiol. 2004; 58:207–216. [PubMed: 14704953]

Hyman BT, Trojanowski JQ. Consensus recommendations for the postmortem diagnosis of Alzheimer disease from the National Institute on Aging and the Reagan Institute Working Group on diagnostic criteria for the neuropathological assessment of Alzheimer disease. J. Neuropathol. Exp. Neurol. 1997; 56:1095–1097. [PubMed: 9329452]

Ibanez CF. Message in a bottle: long-range retrograde signaling in the nervous system. Trends Cell Biol. 2007; 17:519–528. [PubMed: 18029183]

Kaur G, Mohan P, Pawlik M, Derosa S, Fajiculay J, Che S, Grubb A, Ginsberg SD, Nixon RA, Levy E. Cystatin C rescues degenerating neurons in a cystatin B-knockout mouse model of progressive myoclonus epilepsy. Am J Pathol. 2010; 177:2256–2267. [PubMed: 20889561]

Liang WS, Dunckley T, Beach TG, Grover A, Mastroeni D, Walker DG, Caselli RJ, Kukull WA, McKeel D, Morris JC, Hulette C, Schmechel D, Alexander GE, Reiman EM, Rogers J, Stephan DA. Gene expression profiles in anatomically and functionally distinct regions of the normal aged human brain. Physiol Genomics. 2007; 28:311–322. [PubMed: 17077275]

Liang WS, Reiman EM, Valla J, Dunckley T, Beach TG, Grover A, Niedzielko TL, Schneider LE, Mastroeni D, Caselli R, Kukull W, Morris JC, Hulette CM, Schmechel D, Rogers J, Stephan DA. Alzheimer's disease is associated with reduced expression of energy metabolism genes in posterior cingulate neurons. Proc Natl Acad Sci USA. 2008; 105:4441–4446. [PubMed: 18332434]

Licastro F, Chiappelli M. Brain immune responses cognitive decline and dementia: relationship with phenotype expression and genetic background. Mech Ageing Dev. 2003; 124:539–548. [PubMed: 12714265]

Liu J, Lamb D, Chou MM, Liu YJ, Li G. Nerve growth factor-mediated neurite outgrowth via regulation of Rab5. Mol Biol Cell. 2007; 18:1375–1384. [PubMed: 17267689]

Mathews PM, Guerra CB, Jiang Y, Grbovic OM, Kao BH, Schmidt SD, Dinakar R, Mercken M, Hille-Rehfeld A, Rohrer J, Mehta P, Cataldo AM, Nixon RA. Alzheimer's disease-related overexpression of the cation-dependent mannose 6-phosphate receptor increases Abeta secretion: role for altered lysosomal hydrolase distribution in beta-amyloidogenesis. J Biol Chem. 2002; 277:5299–5307. [PubMed: 11551970]

Mirra SS, Heyman A, McKeel D, Sumi SM, Crain BJ, Brownlee LM, Vogel FS, Hughes JP, van Belle G, Berg L, The Consortium to Establish a Registry for Alzheimer's Disease (CERAD). Part II. Standardization of the neuropathologic assessment of Alzheimer's disease. Neurology. 1991; 41:479–486. [PubMed: 2011243]

Mufson EJ, Bothwell M, Hersh LB, Kordower JH. Nerve growth factor receptor immunoreactive profiles in the normal, aged human basal forebrain: colocalization with cholinergic neurons. J Comp Neurol. 1989a; 285:196–217. [PubMed: 2547849]

Mufson EJ, Bothwell M, Kordower JH. Loss of nerve growth factor receptor-containing neurons in Alzheimer's disease: a quantitative analysis across subregions of the basal forebrain. Exp Neurol. 1989b; 105:221–232. [PubMed: 2548888]

Mufson EJ, Counts SE, Fahnestock M, Ginsberg SD. Cholinotrophic molecular substrates of mild cognitive impairment in the elderly. Curr Alzheimer Res. 2007a; 4:340–350. [PubMed: 17908035]

Mufson, EJ.; Counts, SE.; Fahnestock, M.; Ginsberg, SD. NGF family of neurotrophins and their receptors: early involvement in the progression of Alzheimer's disease. In: Dawbarn, D.; Allen,

SJ., editors. Neurobiology of Alzheimer's Disease. Third Edition. Oxford University Press; Oxford: 2007b. p. 283-321.

Mufson EJ, Counts SE, Ginsberg SD. Single cell gene expression profiles of nucleus basalis cholinergic neurons in Alzheimer's disease. Neurochem Res. 2002; 27:1035–1048. [PubMed: 12462403]

Mufson EJ, Counts SE, Perez SE, Ginsberg SD. Cholinergic system during the progression of Alzheimer's disease: therapeutic implications. Expert Rev Neurother. 2008; 8:1703–1718. [PubMed: 18986241]

Mufson EJ, Ginsberg SD, Ikonomovic MD, DeKosky ST. Human cholinergic basal forebrain: chemoanatomy and neurologic dysfunction. J Chem Neuroanat. 2003; 26:233–242. [PubMed: 14729126]

Mufson EJ, Ma SY, Cochran EJ, Bennett DA, Beckett LA, Jaffar S, Saragovi HU, Kordower JH. Loss of nucleus basalis neurons containing trkA immunoreactivity in individuals with mild cognitive impairment and early Alzheimer's disease. J Comp Neurol. 2000; 427:19–30. [PubMed: 11042589]

Mufson EJ, Wuu J, Counts SE, Nykjaer A. Preservation of cortical sortilin protein levels in MCI and Alzheimer's disease. Neurosci Lett. 2010; 471:129–133. [PubMed: 20085800]

Ng EL, Tang BL. Rab GTPases and their roles in brain neurons and glia. Brain Res Rev. 2008; 58:236–246. [PubMed: 18485483]

Nixon RA. Niemann-Pick Type C disease and Alzheimer's disease: the APP-endosome connection fattens up. Am J Pathol. 2004; 164:57–761.

Nixon RA, Cataldo AM. The endosomal-lysosomal system of neurons: new roles. Trends Neurosci. 1995; 18:489–496. [PubMed: 8592758]

Nixon RA, Cataldo AM. Lysosomal system pathways: genes to neurodegeneration in Alzheimer's disease. J Alzheimers Dis. 2006; 9:277–289. [PubMed: 16914867]

Nixon RA, Cataldo AM, Mathews PM. The endosomal-lysosomal system of neurons in Alzheimer's disease pathogenesis: a review. Neurochem Res. 2000; 25:1161–1172. [PubMed: 11059790]

Nixon RA, Mathews PM, Cataldo AM. The neuronal endosomal-lysosomal system in Alzheimer's disease. J Alzheimers Dis. 2001; 3:97–107. [PubMed: 12214078]

Nixon RA, Yang DS, Lee JH. Neurodegenerative lysosomal disorders: a continuum from development to late age. Autophagy. 2008; 4:590–599. [PubMed: 18497567]

Novick P, Brennwald P. Friends and family: the role of the Rab GTPases in vesicular traffic. Cell. 1993; 75:597–601. [PubMed: 8242735]

Ostrowski M, Carmo NB, Krumeich S, Fanget I, Raposo G, Savina A, Moita CF, Schauer K, Hume AN, Freitas RP, Goud B, Benaroch P, Hacohen N, Fukuda M, Desnos C, Seabra MC, Darchen F, Amigorena S, Moita LF, Thery C. rab27a and rab27b control different steps of the exosome secretion pathway. Nat Cell Biol. 2010; 12:19–30. [PubMed: 19966785]

Peng S, Wuu J, Mufson EJ, Fahnestock M. Increased proNGF levels in subjects with mild cognitive impairment and mild Alzheimer disease. J Neuropathol Exp Neurol. 2004; 63:641–649. [PubMed: 15217092]

Peng S, Wuu J, Mufson EJ, Fahnestock M. Precursor form of brain-derived neurotrophic factor and mature brain-derived neurotrophic factor are decreased in the pre-clinical stages of Alzheimer's disease. J Neurochem. 2005; 93:1412–1421. [PubMed: 15935057]

Petersen RC, Negash S. Mild cognitive impairment: an overview. CNS Spectr. 2008; 13:45–53. [PubMed: 18204414]

Reisberg B, Ferris SH, Kluger A, Franssen E, Wegiel J, de Leon MJ. Mild cognitive impairment (MCI): a historical perspective. Int Psychogeriatr. 2008; 20:18–31. [PubMed: 18031593]

Salehi A, Delcroix JD, Belichenko PV, Zhan K, Wu C, Valletta JS, Takimoto-Kimura R, Kleschevnikov AM, Sambamurti K, Chung PP, Xia W, Villar A, Campbell WA, Kulnane LS, Nixon RA, Lamb BT, Epstein CJ, Stokin GB, Goldstein LS, Mobley WC. Increased App expression in a mouse model of Down's syndrome disrupts NGF transport and causes cholinergic neuron degeneration. Neuron. 2006; 51:29–42. [PubMed: 16815330]

SAS Institute Inc. Proc Mixed in SAS® software. SAS Publishing; Cary, NC: 2009.

Saxena S, Bucci C, Weis J, Kruttgen A. The small GTPase Rab7 controls the endosomal trafficking and neuritogenic signaling of the nerve growth factor receptor TrkA. J Neurosci. 2005; 25:10930–10940. [PubMed: 16306406]

Schatteman GC, Gibbs L, Lanahan AA, Claude P, Bothwell M. Expression of NGF receptor in the developing and adult primate central nervous system. J Neurosci. 1988; 8:860–873. [PubMed: 2831315]

Seachrist JL, Ferguson SS. Regulation of G protein-coupled receptor endocytosis and trafficking by Rab GTPases. Life Sci. 2003; 74:225–235. [PubMed: 14607250]

Spang A. Vesicle transport: a close collaboration of Rabs and effectors. Curr Biol. 2004; 14:R33–34. [PubMed: 14711434]

Valdez G, Philippidou P, Rosenbaum J, Akmentin W, Shao Y, Halegoua S. Trk-signaling endosomes are generated by Rac-dependent macroendocytosis. Proc Natl Acad Sci USA. 2007; 104:12270–12275. [PubMed: 17640889]

Wang B, Yang L, Wang Z, Zheng H. Amyolid precursor protein mediates presynaptic localization and activity of the high-affinity choline transporter. Proc Natl Acad Sci USA. 2007; 104:14140–14145. [PubMed: 17709753]

Whitehouse PJ, Price DL, Struble RG, Clark AW, Coyle JT, Delong MR. Alzheimer's disease and senile dementia: loss of neurons in the basal forebrain. Science. 1982; 215:1237–1239. [PubMed: 7058341]

Winblad B, Palmer K, Kivipelto M, Jelic V, Fratiglioni L, Wahlund LO, Nordberg A, Backman L, Albert M, Almkvist O, Arai H, Basun H, Blennow K, de Leon M, DeCarli C, Erkinjuntti T, Giacobini E, Graff C, Hardy J, Jack C, Jorm A, Ritchie K, van Duijn C, Visser P, Petersen RC. Mild cognitive impairment--beyond controversies, towards a consensus: report of the International Working Group on Mild Cognitive Impairment. J Intern Med. 2004; 256:240–246. [PubMed: 15324367]

Zerial M, Stenmark H. Rab GTPases in vesicular transport. Curr Opin Cell Biol. 1993; 5:613–620. [PubMed: 8257602]

RESEARCH HIGHLIGHTS

Microarrays, qPCR, and immunoblotting assessed CBF neurons in NCI, MCI and AD.

Upregulation of select rab GTPases was seen in MCI and AD versus NCI CBF neurons.

Upregulation of rab4, rab5, rab7 and rab27 was validated via qPCR in basal forebrain.

rab GTPase defects correlated with antemortem cognitive decline and neuropathology.

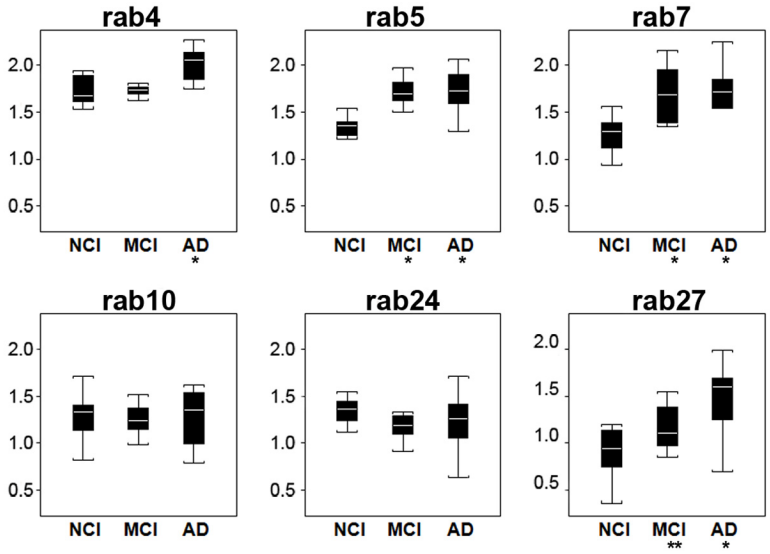

Figure 1.

Differential regulation of rab GTPases during the progression of AD. Box and whisker plots indicating log-transformed gene expression levels of select rab GTPases. Upregulation of *rab5* and *rab7* was found in MCI and AD (asterisks) and is considered an early change. Upregulation of *rab4* was seen in AD (asterisk) and is considered a later change. *rab27* upregulation in MCI (double asterisk) was considered intermediate between NCI and AD (asterisk).

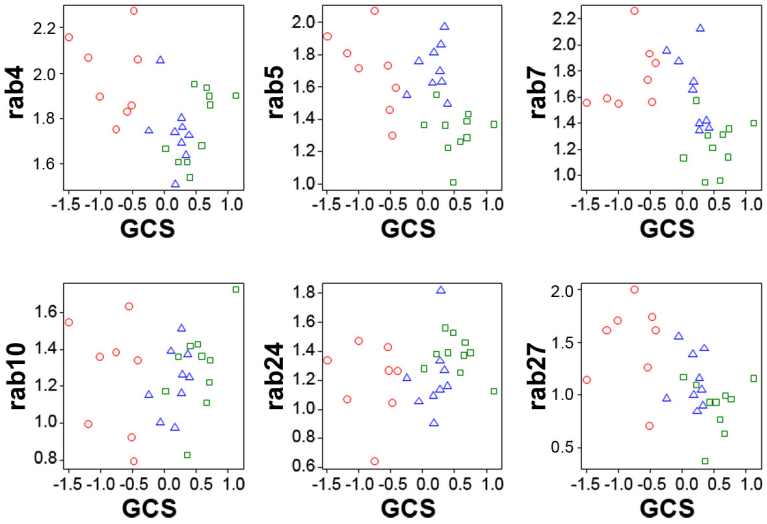

Figure 2.

Association between select rab GTPase gene expression levels within CBF neurons and antemortem cognitive measures in the same subjects. Scatterplots illustrate the association between gene expression levels and GCS for cases classified as AD (red circles), MCI (blue triangles), and NCI (green squares). Strong negative associations were observed between *rab4* ($p < 0.02$), *rab5* ($p < 0.004$), *rab7* ($p < 0.006$), and *rab27* ($p < 0.004$) gene expression and GCS performance. No significant associations were observed between *rab10* and *rab24* expression and GCS.

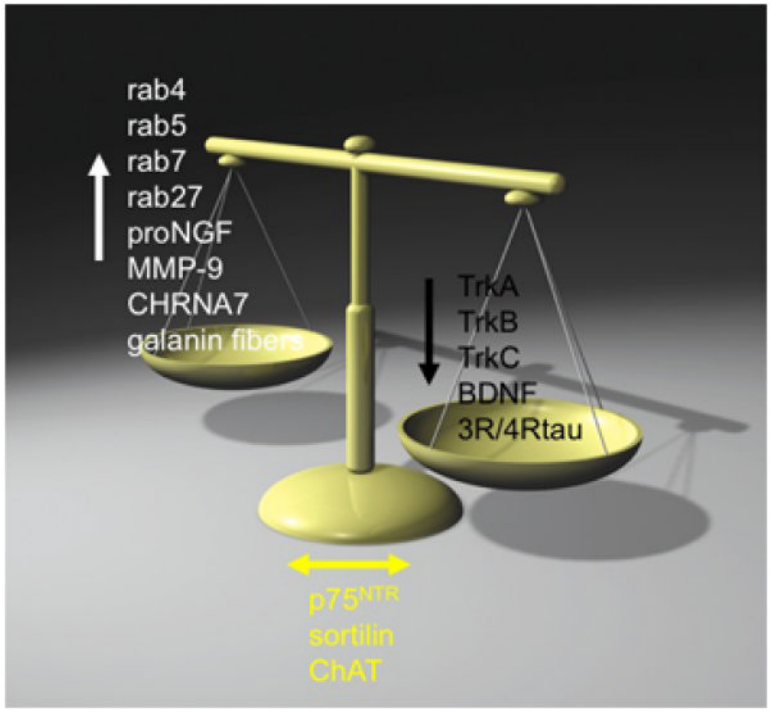

Figure 3.
Schematic illustrating the balance between specific genes and encoded proteins that are altered in vulnerable CBF neurons during the progression of AD. Specific elements that have been found to be upregulated (white), downregulated (black), and not significantly altered (yellow) are depicted which may contribute to the selective vulnerability of NB neurons. Adapted from (Mufson *et al.*, 2008).

J Chem Neuroanat. Author manuscript; available in PMC 2012 October 1.

Table I

Microarray analysis: clinical, demographic, and neuropathological characteristics by diagnosis category

		Clinical Diagnosis			Comparison by diagnosis group	Pair-wise comparisons*
		NCI (n=11)	MCI (n=10)	AD (n=9)		
Age at death (years)	Mean ± SD (range)	81.0 ± 9.6 (66-92)	81.9 ± 4.3 (75-92)	86.6 ± 4.8 (80-94)	p = 0.2[a]	-
Number (%) of males		5 (45%)	6 (40%)	2 (29%)	p = 0.6[b]	-
Educational level	Mean ± SD (range)	17.6 ± 5.0 (8-24)	18.8 ± 2.3 (16-22)	16.3 ± 4.1 (6-20)	p = 0.4[a]	-
MMSE	Mean+SD (range)	27.6 ± 1.6 (25-30)	26.6 ± 2.8 (20-30)	20.0 ± 4.5 (14-25)	p < 0.0001[a]	(NCI & MCI) > AD
GCS	Mean±SD (range)	0.5+0.3 (0.0-1.1)	0.2+0.2 (-0.2, 0.4)	−0.8 ± 0.4 (−1.5, −0.4)	p < 0.0001[a]	(NCI & MCI) > AD
ApoE ε4 allele (%)		2 (18%)	6 (40%)	6 (86%)	p < 0.07[b]	-
PMI (hours)	Mean±SD (range)	12.1 ± 11.2 (3.2-33.5)	7.8±4.7 (3.6-16)	7.3±4.1 (2.2-12)	p = 0.2[a]	-
Distribution of Braak scores:	0 I/II III/IV V/VI	1 4 6 0	0 0 8 2	0 1 3 5	p < 0.003[c]	NCI < (MCI & AD)
Distribution of NIA Reagan diagnosis (likelihood of AD)	No AD Low Intermediate High	0 6 4 0	0 3 7 0	0 1 4 4	p < 0.01[c]	NCI < AD
CERAD diagnosis	No AD Possible Probable Definite	5 1 3 1	1 2 3 4	0 0 5 4	p < 0.02[c]	NCI < AD

[a] One-way ANOVA

[b] Fisher's exact test

[c] Kruskal-Wallis test

* With Bonferroni correction

Table II

rab GTPase expression levels (via microarray analysis) by disease category (mean ± SEM)

	Clinical Diagnosis			Comparison by diagnosis group*		Pair-wise comparisons*
	NCI (n=11)	MCI (n=10)	AD (n=9)			
rab4	5.94 ± 0.29	5.82 ± 0.30	7.63 ± 0.34	$F_{(2,24.9)} = 9.6$	$p < 0.0008$	(NCI & MCI) < AD
rab5	3.86 ± 0.26	5.72 ± 0.27	5.80 ± 0.31	$F_{(2,24.9)} = 18.5$	$p < 0.0001$	NCI < (MCI & AD)
rab7	3.67 ± 0.41	5.81 ± 0.43	6.02 ± 0.47	$F_{(2,27.3)} = 11.7$	$p < 0.0002$	NCI < (MCI & AD)
rab10	3.84 ± 0.25	3.84 ± 0.26	4.10 ± 0.29	$F_{(2,129)} = 0.3$	$p = 0.7$	-
rab24	4.11 ± 0.21	3.67 ± 0.22	3.79 ± 0.25	$F_{(2,129)} = 1.4$	$p = 0.3$	-
rab27	2.70 ± 0.31	3.36 ± 0.32	4.59 ± 0.34	$F_{(2,24.2)} = 8.2$	$p < 0.002$	NCI < AD
rab1	2.19 ± 0.18	2.76 ± 0.18	2.32 ± 0.22	$F_{(2,26.6)} = 2.7$	$p = 0.08$	-
rab3	2.79 ± 0.24	2.65 ± 0.25	2.19 ± 0.28	$F_{(2,21.1)} = 2.3$	$p = 0.1$	-
rab2	2.10 ± 0.14	2.32 ± 0.14	2.12 ± 0.17	$F_{(2,30.8)} = 0.7$	$p = 0.5$	-
rab6	2.46 ± 0.18	2.59 ± 0.18	3.17 ± 0.21	$F_{(2,123)} = 2.6$	$p = 0.08$	-

*Mean and standard error were estimated using mixed models analysis for repeated measures

**Log-transformed gene expression values were used for comparison

Table III

rab GTPase expression levels via qPCR analysis by disease category (mean ± SD)

	Clinical Diagnosis			Comparison by diagnosis group*	Pair-wise comparisons**
	NCI (n=11)	MCI (n=8)	AD (n=8)		
rab4	4.6 ± 0.2	4.6 ± 0.3	5.4 ± 0.3	$p < 0.0005$	(NCI & MCI) < AD
rab5	4.6 ± 0.1	4.6 ± 0.1	5.2 ± 0.2	$p < 0.0003$	(NCI & MCI) < AD
rab7	4.6 ± 0.2	5.0 ± 0.1	5.4 ± 0.4	$p < 0.0001$	NCI < (MCI & AD)
rab24	4.6 ± 0.2	4.7 ± 0.2	4.9 ± 0.3	$p < 0.09$	-
rab27	4.6 ± 0.3	4.6 ± 0.2	5.2 ± 0.4	$p < 0.002$	(NCI & MCI) < AD

*Kruskal-Wallis test

**With Bonferroni correction

Table IV

rab5 and rab7 protein levels via immunoblot analysis by disease category (mean±SD)

	Clinical Diagnosis				
	NCI (n=18)	**MCI (n=10)**	**AD (n=17)**	**Comparison by diagnosis group***	**Pair-wise comparisons***
rab5	0.90±0.17	1.10±0.19	1.14±0.17	$p < 0.02^a$	NCI < (MCI & AD)
rab7	0.99±0.11	1.07±0.12	1.09±0.14	$p < 0.09^a$	-

[a] Kruskal-Wallis test

* With Bonferroni correction